

An improved experimental setup for high-resolution vacuum ultraviolet laser spectroscopy

Christine M. Steenkamp^{*†}, Anton du Plessis^{*} and Erich G. Rohwer^{*}

The experimental setup for vacuum ultraviolet (VUV) laser spectroscopy at Stellenbosch University's Laser Research Institute, has been improved by the addition of a VUV monochromator. The VUV source has been characterized over the extended wavelength range 144.2–157.7 nm, and simultaneous measurement of laser-induced fluorescence and absorption spectra has been achieved. We discuss current investigations of carbon monoxide molecules and complexes, facilitated by the narrow bandwidth of the VUV light and the low temperature collision-free conditions in a supersonic jet.

Introduction

This paper reports on the latest developments in vacuum ultraviolet (VUV) laser spectroscopy at Stellenbosch University's Laser Research Institute. Recent modifications, making the setup more versatile and allowing an improved characterization of the VUV source, are described. Our investigations on carbon monoxide (CO) molecules and complexes are discussed to illustrate the potential of the equipment for future interdisciplinary applications.

The VUV region of the optical spectrum, constituting the wavelength range 100–200 nm, is relevant to many scientific disciplines. VUV light facilitates the investigation of the electronic excitation spectra of small molecules important in astrophysics (CO, NO, H₂, N₂)^{1,2} and allows photo-dissociation and soft, one-photon ionization of larger molecules in analytical chemistry.³ VUV radiation is used to investigate the optoelectronic characteristics and photo-induced degradation of large band gap materials such as fused silica and diamond.^{4,5} The use of ever shorter wavelengths in the lithographic production of electronic circuits motivates applied research in the VUV.⁶ Despite these reasons, the VUV region has not been explored as extensively by laser spectroscopy as the visible and infrared regions due to lack of commercial VUV sources that provide continuously tunable, narrow-bandwidth light.

In our experimental setup, two specialized techniques are combined: the generation of narrow bandwidth, tunable coherent VUV by a nonlinear optical process in a gaseous medium and the flow-cooling of the spectroscopic sample in a supersonic jet.^{7,8} We describe here the physical principles of these techniques, the characteristics of the experimental setup and how it is currently used.

Physical principles of the techniques

The VUV source

Four-wave mixing — referred to as sum or difference frequency mixing — is a widely used process for generating narrow band-

width, tunable VUV radiation. As nonlinear crystals are opaque in the largest part of the VUV region,⁹ gaseous nonlinear media are used.¹⁰ Metal vapours are attractive for frequency mixing due to their high nonlinear susceptibility. For a recent review of VUV generation techniques, refer to Eden.¹¹

The specific four-wave mixing process employed in our setup is the interaction of high-power visible laser pulses at frequencies ν_1 and ν_2 with a magnesium vapour medium to generate VUV light at the sum frequency $\nu_{\text{SF}} = 2\nu_1 + \nu_2$. The susceptibility for the conversion process is greatly enhanced by a two-photon resonance of ν_1 with the $3s^2\ ^1S - 3s3d\ ^1D$ transition of magnesium. The VUV sum-frequency wavelength is tuned continuously by tuning ν_2 . In addition to the sum-frequency light, some VUV radiation at the fixed third harmonic frequency, $\nu_{\text{TH}} = 3\nu_1$, is generated in the setup.

The efficiency of the sum-frequency generation is optimized by phase matching. In the case of a magnesium vapour medium, this is achieved by adding krypton gas. The incident beams are circularly polarized to optimize further the generation of the sum-frequency light. More details on phase matching and polarization requirements in VUV generation can be found elsewhere.^{10,12}

Flow-cooling in a supersonic jet

A supersonic jet is formed by allowing a gas, often an inert atomic carrier gas seeded with the analyte molecules, to expand from a high-pressure reservoir through a small nozzle orifice into vacuum. The use of the seeded supersonic jet in spectrometry has been reviewed recently.³ In the initial phase of the expansion, the numerous collisions convert the random thermal motion of the gas particles into directed mass flow, causing a rapid decrease in the translational temperature of the gas.¹³ The cooling of the rotational and vibrational degrees of freedom of the analyte molecules in the jet depends on energy transfer between the different degrees of freedom and takes place at lower rates. As the expansion proceeds, the flow-cooling combined with the decrease in the gas density results in cold and collision-free conditions.

The extent of condensation in a supersonic jet is limited and can be controlled by experimental conditions.¹³ This makes a supersonic jet suitable for the formation of small van der Waals complexes.¹⁴

Experimental setup

The basic equipment⁷ has been modified by the implementation of a VUV monochromator (McPherson Model 218) evacuated by a diffusion pump (Edwards Diffstak 63). The modified setup is illustrated in Fig. 1.

The incident laser beams are provided by two dye lasers (Lambda Physik FL 3001 X, up to 2 mJ per 20-ns pulse) pumped by the same XeCl excimer laser (Lambda Physik EMG 203 MSC, 150 mJ per 25-ns pulse). The phase-matched nonlinear medium of magnesium vapour and krypton gas is prepared in the heat pipe oven.^{12,7} The generated VUV beam crosses the supersonic jet approximately 25 nozzle diameters from the nozzle.

The supersonic jet is pulsed using a solenoid valve (General Valves Series 9) synchronized with the laser pulses by a delay generator (Stanford Research Systems, DG 535). A recently acquired valve driver (Iota One Pulse Driver, General Valve Corporation) produces gas pulses of 0.8 ms and allows repetition rates of up to 10 Hz without increasing the chamber pressure, maintained at $c. 5 \times 10^{-5}$ mbar. Gas mixtures varying from 0.5% CO in a carrier gas (Ar or Ne) to 100% CO are used, expanding from pressures of typically 3–4 bar. Different gas mixtures and

^{*}Laser Research Institute, Physics Department, University of Stellenbosch, Private Bag X1, Matieland 7602, South Africa.

[†]Author for correspondence. E-mail: cmsteen@sun.ac.za

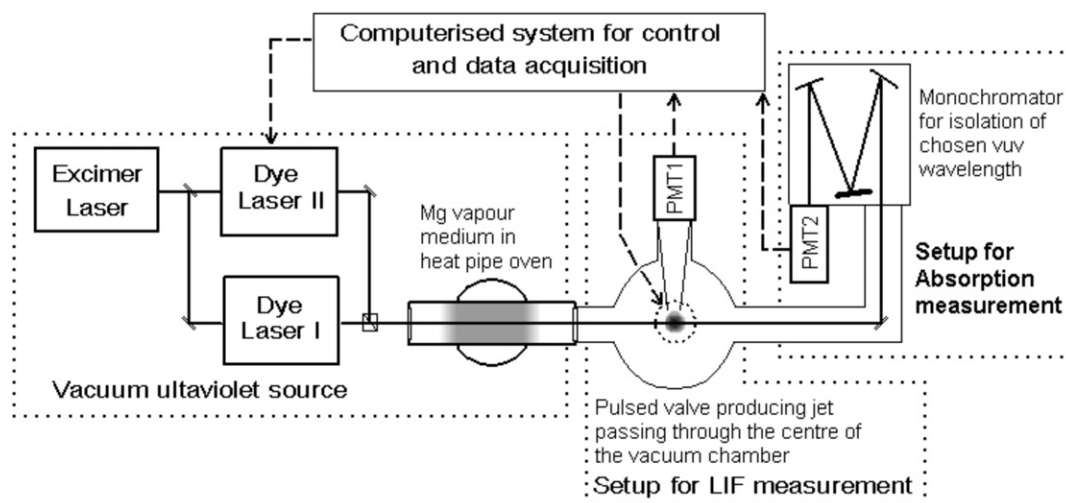


Fig. 1. Schematic illustration of the experimental setup. The dotted lines indicate the different functional parts of the equipment. The dashed lines indicate connections between the equipment and the control and data acquisition systems.

pressures are used to control the temperature of the sample.

The monochromator is applied as in Fig. 1 to separate the two VUV wavelengths generated — the sum-frequency and the third harmonic frequency — in the transmitted beam, allowing their separate measurement by the solarblind photomultiplier, PMT2 (Hamamatsu R973). Simultaneously, the undispersed laser-induced fluorescence (LIF) from the irradiated sample volume is measured by another solarblind photomultiplier, PMT1 (EMR Electronic 542G). Alternatively, the monochromator is connected at the PMT1 position to collect the fluorescence spectrum.

Characterization of the setup

Using the monochromator, the VUV source was characterized over an extended wavelength range. Figure 2 shows the VUV power over the range 144.2–157.7 nm. The power of the sum-frequency light is wavelength dependent; the dips in power are due to increased absorption near auto-ionizing levels of the atomic magnesium.¹⁰ The fluctuations in sum-frequency power do not influence the third harmonic power at 143.6 nm, which is constant within *c.* 5% over a tuning range, given a constant power of the ν_1 dye laser. This proves that the generation of the third harmonic and sum-frequency wavelengths are independent processes in the intensity regime of our experiment. Over the extended tuning range the spectral bandwidth of the sum-frequency is smaller than 0.4 cm^{-1} and the estimated maximum peak power is in the order of 5 mW. The peak power depends strongly on the power of the dye lasers and the phase matching.

In each wavelength region the krypton pressure needed for optimal phase matching differs. Typical results (Fig. 3) show that a krypton pressure of 33 kPa optimizes sum-frequency generation at 148.7 nm, whereas the optimal pressure for third harmonic generation is 29 kPa.

Simultaneously measured LIF and absorption spectra of CO were achieved and are illustrated in Fig. 4. The signal-to-noise ratio is $>500:1$ for the fluorescence spectrum and $\sim 10:1$ for the absorption spectrum.

The advantage of the low temperature achieved in the jet is illustrated in Fig. 5. At rotational temperatures below 10 K the population of the CO molecules is practically confined to the lowest few rotational levels, enhancing the relative intensities of the low-*J* spectral lines. This simplifies the spectrum and results in a low detection limit; 3 parts per million for CO.¹⁵

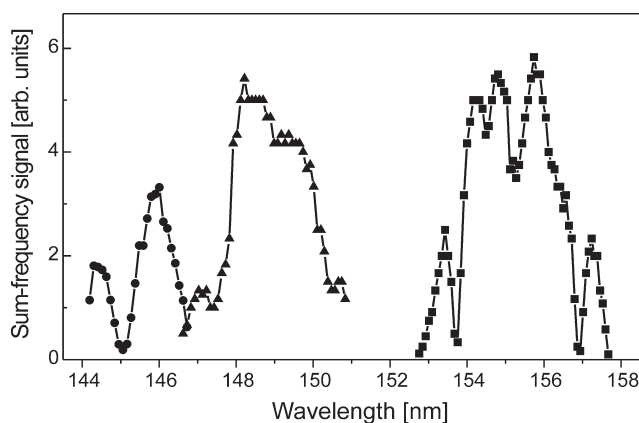


Fig. 2. The sum-frequency signal over the tuning ranges covered by three different laser dyes in the laser providing frequency ν_2 : Coumarin 440 (circles), Coumarin 480 (triangles) and Coumarin 540 (squares). The curves were normalized to compensate for different monochromator slit widths used. The scale on the y-axis represents a rough estimate of the peak power in mW.

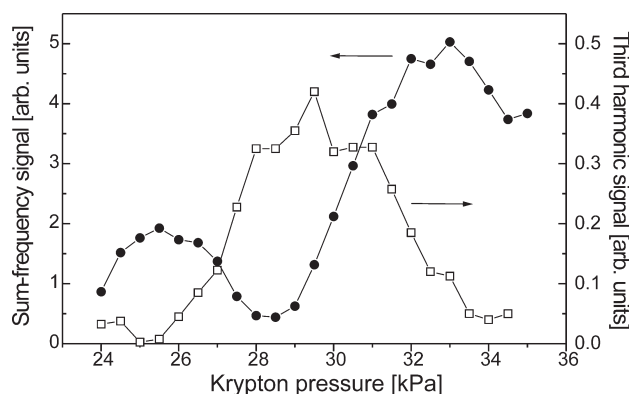


Fig. 3. Phase-matching curves for the generation of the sum-frequency radiation at 148.7 nm (solid dots) and the third harmonic at 143.6 nm (open squares). The y-axis scale represents a rough estimate of the peak power in mW plotted against the partial pressure of the krypton gas in the medium at a constant magnesium vapour pressure of 1 kPa.

Current spectroscopy applications

The $A^1\Pi-X^1\Sigma^+$ band of CO, an important feature of astrophysical observations,¹ has been well characterized for $^{12}\text{C}^{16}\text{O}$ (98.7% in nature), $^{13}\text{C}^{16}\text{O}$ (1.1%) and $^{12}\text{C}^{18}\text{O}$ (0.2%), but for the $^{12}\text{C}^{17}\text{O}$ isotopomer (0.038%) laboratory-measured wavelengths for the rovibronic lines are largely lacking.¹⁶

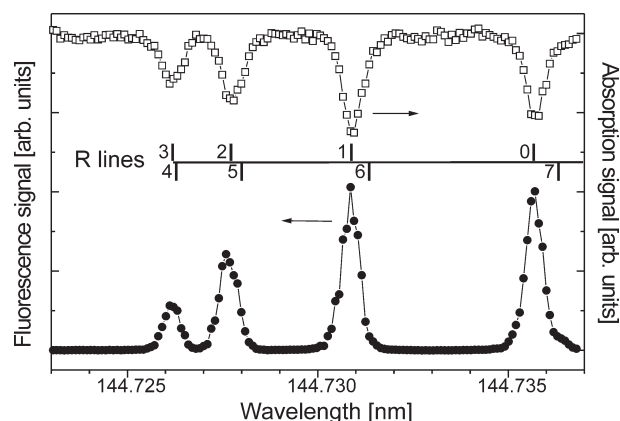


Fig. 4. Simultaneously measured fluorescence (solid diamonds) and absorption spectra (open squares) showing detail of the lowest R-branch rotational lines of the $\text{C}^{12}\text{O}^{16}\text{A}^1\Pi(v' = 3) - \text{X}^1\Sigma^+(v'' = 0)$ band.

As a first application, the rotationally resolved LIF spectrum of the $\text{A}^1\Pi(v' = 3) - \text{X}^1\Sigma^+(v'' = 0)$ vibrational band of a flow-cooled natural CO gas sample was recorded. As previously reported in detail,¹⁷ these measurements produced the first laboratory-measured wavelengths for the $^{12}\text{C}^{17}\text{O}$ isotopomer, which were applicable to the interpretation of astrophysical data. This work is currently being extended to the $\text{A}^1\Pi(v') - \text{X}^1\Sigma^+(v'' = 0)$ vibrational bands with $v' = 0-5$. Figure 6 shows recently acquired LIF spectra of the $v' = 0-3$ bands containing lines of all four isotopomers. It should be possible to extract new $^{12}\text{C}^{17}\text{O}$ wavelength data from these spectra.

In the active research field of van der Waals complexes, $\text{CO} \cdots \text{CO}$ dimers and $\text{CO} \cdots \text{rare gas}$ complexes feature as prototype species, for which there is a lack of experimental data on their electronically excited states.¹⁸

An ongoing investigation is aimed at measuring the electronic excitation spectrum of $\text{CO} \cdots \text{R}$ (R being Ar or Ne) and $\text{CO} \cdots \text{CO}$. We previously presented evidence for the formation of these CO-containing van der Waals complexes in the supersonic jet, but an absence of spectral features of the complexes in the LIF spectra.¹⁵ Absorption spectra will be useful to detect non-fluorescing complex species.

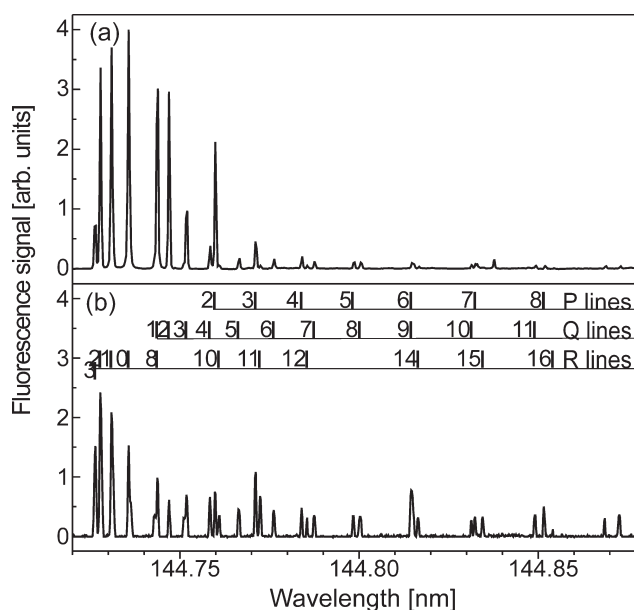


Fig. 5. Detail of the $\text{C}^{12}\text{O}^{16}\text{A}^1\Pi(v' = 3) - \text{X}^1\Sigma^+(v'' = 0)$ vibrational band measured (a) at 10 K and (b) at approximately 100 K. The spectra are normalized to represent the same sample density.

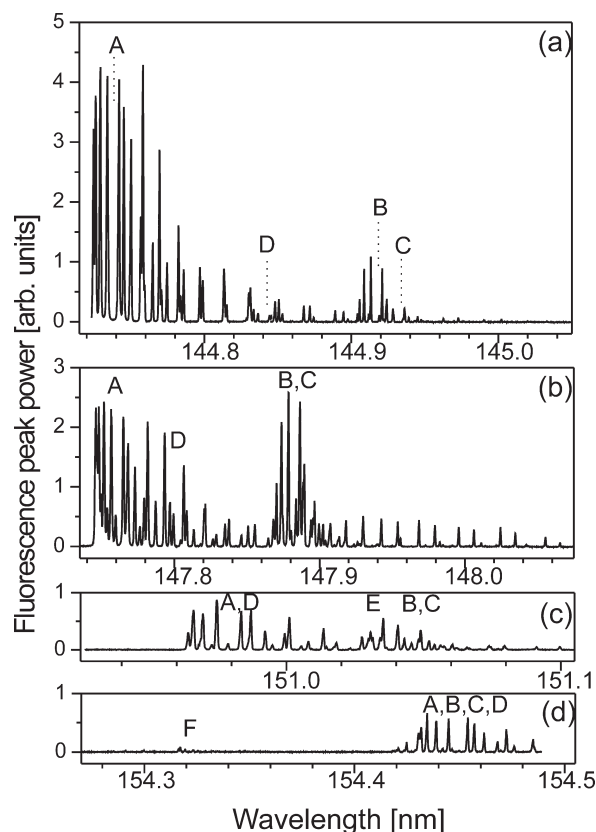


Fig. 6. Spectra of the $\text{A}^1\Pi(v') - \text{X}^1\Sigma^+(v'' = 0)$ vibrational bands of CO with (a) $v' = 3$, (b) $v' = 2$, (c) $v' = 1$, (d) $v' = 0$ measured in a sample of pure CO gas expanded from a pressure of 4 bar. The wavelength calibration is preliminary. Lines of the $\text{A}^1\Pi(v') - \text{X}^1\Sigma^+(v'' = 0)$ bands of $^{12}\text{C}^{16}\text{O}$ (A), $^{13}\text{C}^{16}\text{O}$ (B), $^{12}\text{C}^{18}\text{O}$ (C) and $^{12}\text{C}^{17}\text{O}$ (D), as well as the forbidden transitions $d^3\Delta_1(v' = 5) - \text{X}^1\Sigma^+(v'' = 0)$ (E) and $e^3\Sigma^-(v' = 1) - \text{X}^1\Sigma^+(v'' = 0)$ (F) of $^{12}\text{C}^{16}\text{O}$ are expected to be observable. Dotted lines in (a) indicate band origins.

Conclusions and outlook

The first applications of the facility for VUV laser spectroscopy on CO molecules and complexes demonstrated the high spectral resolution and low detection limit attainable in LIF spectroscopy, resulting from the narrow bandwidth and high spectral brightness of the VUV source, as well as the low-temperature, collision-free conditions in the supersonic jet. Improved characterization of the VUV source facilitated by the monochromator confirmed that sum-frequency and third harmonic generation are independent in the power regime of this experiment. Simultaneous absorption and fluorescence measurements have also been demonstrated. This may facilitate the detection of non-fluorescing species.

Future work with this equipment aims at improving the signal-to-noise ratio in the absorption spectra and increasing the amount of fluorescence collected to facilitate the detection of dispersed fluorescence spectra.

Future investigations will include spectroscopy on selected Si-O containing molecules, and applications of soft one-photon ionization with a time-of-flight mass spectrometer as detector. Possible interdisciplinary applications could include investigation of VUV-induced degradation of fused silica or other large band gap materials and analysis of biological samples by photo-ionization.

This research was supported by the CSIR National Laser Centre. A. du Plessis acknowledges financial support from the Department of Labour.

1. Balser D.S., McMullin J.P. and Wilson T.L. (2002). CO isotopes in planetary nebulae. *Astrophys. J.* 572, 326–334.

2. Knauth D.C., Andersson B.-G., McCandliss S.R. and Moos H.W. (2004). The interstellar N₂ abundance towards HD 124314 from far-ultraviolet observations. *Nature* **429**, 636–638.
3. Imasaka T., Moore D.S. and Vo-Dinh T. (2003). Critical assessment: use of supersonic jet spectrometry for complex mixture analysis. *Pure Appl. Chem.* **75**, 975–998.
4. Hosono H., Ikuta Y., Kinoshita T., Kajihara K. and Hirano M. (2001). Physical disorder and optical properties in the vacuum ultraviolet region of amorphous SiO₂. *Phys. Rev. Lett.* **87**, 175501.
5. Miskys C.R., Garrido J.A., Hermann M., Eickhoff M., Nebel C.E., Stutzmann M. and Vogg G. (2004). Structural and interface properties of an AlN diamond ultraviolet light emitting diode. *Appl. Phys. Lett.* **85**, 3699–3701.
6. Neukirch U. and Li X.H. (2004). High-accuracy measurement of the optical transmittance of optical bulk materials at deep-ultraviolet wavelengths. *Appl. Opt.* **43**, 3978–3982.
7. Du Plessis A., Steinmann C.M. and Rohwer E.G. (2005). Experimental parameters in vacuum ultraviolet laser spectroscopy. *S. Afr. J. Sci.* **101**, 93–95.
8. Steinmann C.M. (2003). *Vacuum ultraviolet laser spectroscopy of CO molecules in a supersonic jet*, pp. 19–52. Ph.D. dissertation, University of Stellenbosch.
9. Chen C. (2004). Recent advances in deep and vacuum-UV harmonic generation with KBBF crystal. *Opt. Mat.* **26**, 425–429.
10. Yamanouchi K. and Tsuchiya S. (1995). Tunable vacuum ultraviolet laser spectroscopy: excited state dynamics of jet-cooled molecules and van der Waals complexes. *J. Phys. B At. Mol. Opt. Phys.* **28**, 133–165.
11. Eden J.G. (2000). From N₂ (337 nm) to high-order harmonic generation: 40 years of coherent source development in the UV and VUV. *IEEE Journal on selected topics in quantum electronics* **6**(6), 1051–1060.
12. Steinmann C.M. (1999). *Development and characterisation of a tunable laser source in the vacuum ultraviolet*, pp. 51–99. M.Sc. thesis, University of Stellenbosch.
13. Smalley R.E., Wharton L. and Levy D.H. (1977). Molecular optical spectroscopy with supersonic beams and jets. *Acc. Chem. Res.* **10**, 139–145.
14. Hagen O.F. (1974). Cluster beams from nozzle sources. In *Molecular Beams and Low Density Gasdynamics*, ed. P.P. Wegener, pp. 93–181. Marcel Dekker, New York.
15. Steinmann C.M., Du Plessis A. and Rohwer E.G. (2005). High-resolution vacuum ultraviolet laser spectroscopy of molecules in a free supersonic jet: in search of rare CO isotopomers and CO–Ar van der Waals molecules. *S. Afr. J. Sci.* **101**, 87–88.
16. Sheffer Y., Lambert D.L. and Federman S.R. (2002). Ultraviolet detection of interstellar ¹²C¹⁷O and the CO isotopomeric ratios toward X Persei. *Astrophys. J.* **574**, L171–L174.
17. Steinmann C.M., Rohwer E.G. and Stafast H. (2003). Accurate laboratory wavelengths of the vacuum ultraviolet A(v' = 3)–X(v'' = 0) band of ¹²C¹⁷O and ¹²C¹⁸O. *Astrophys. J.* **590**, L123–L126. Erratum: *Astrophys. J.* **591**, L167.
18. Salazar M.C., Paz J.L., Hernández A.J. and Castejón H.J. (2001). Test study on the excitation spectra of the CO–He van der Waals molecule. *J. Mol. Struct. (THEOCHEM)* **539**, 119–126.